SIMULATION AND EXPERIMENTAL STUDIES ON THE DIABATICITY OF A DIRECT INJECTION DIESEL ENGINE

R. Udayakumar[1] and S.Sundaram[2]
[1]Department of Mechanical Engineering,
[2]Department of Chemical Engineering,
Regional Engineering College,
Tiruchirappalli,
INDIA – 620 015.

Abstract The aim of this research work is to formulate a computer aided simulation code for prediction of combustion & performance parameters and emissions of a Low Heat Rejection Direct Injection Diesel Engine. The low heat rejection (LHR) engines are one in which the combustion chamber walls are coated with high strength ceramic materials, so that the heat losses to the cooling medium is reduced. Four simulation studies are performed with different coating materials like Silicon Carbide, Silicon Nitride, partially stabilized Zirconia's with Magnesium Oxide and partially stabilized Zirconia with Yittria. A sophisticated CI engine test rig has been established as part of the research work and experimental work is carried out on a direct injection diesel engine with a ceramic coating of Zirconia (ZrO) 92% and Yttria (Y_2O_3) 8% to verify the effectiveness of the computer code developed and to analyze the performance of the LHR engines.

Key words: Diesel engine-adiabaticity-computer simulation

INTRODUCTION

The low heat rejection (LHR) engines are one in which the combustion chamber walls are coated with high strength ceramic materials, so that the heat losses to the cooling medium is reduced. Ceramic mechanical properties and ceramic design technology have improved to the point that we can use ceramic as structural part of engines. Low thermal conductivity ceramics can be used to control temperature distribution and heat flow in the structure. When the ceramics are used as the inner surface material of the cylinder, they can reduce the heat transfer between working fluid and walls.

Extensive work [Godfrey, D.J. (1974), Kamo and Bryzik (1981), Jeffrey Carr and Jack Jones (1984), Sekar et al., (1984), Woods (1984), Wurm et al. (1984)] has been done to utilize adiabatic material to improve thermal efficiency by reducing heat losses and to improve mechanical efficiency by eliminating cooling systems. When cylinder-cooling loss is reduced, more of the heat is delivered to the exhaust system. Even without heat recovery system, some of heat is converted to piston work, which increases the thermal efficiency. However installing heat recovery system needs considerable effort, a lot of changes are necessary in the engine configuration. Efficient recovery of energy in the exhaust further improves the thermal efficiency of adiabatic engine.

*Email: uday@rect.ernet.in

The actual diesel engine processes deviate very much from the theoretical cycles. In ideal cycle, the combustion is assumed to be at constant pressure and instantaneous without ignition delay, whereas in actual conditions it is progressive. In ideal cycle, air is assumed to be the working fluid, whereas in real engines it is a mixture of air and fuel. The engine performance parameters like the thermal efficiency & power output of ideal cycles do not match with the values for real engines. Since combustion is the most important phenomenon on which engine performance depends, it is inevitable to analyze the combustion process in detail taking into account the actual working conditions.

SIMULATION WITH TWO ZONE COMBUSTION MODEL

General Description

In this model, the entire cylinder volume is divided into two zones, namely, the burning zone and non-burning zone. The spray zone is identified as burning zone and the rest of the portion of cylinder as non-burning zone. The fuel is introduced into the combustion chamber of a diesel engine through the nozzle with a large pressure differential between the fuel supply line and the cylinder. As the liquid jet leaves the nozzle, it becomes turbulent and spreads out as it entrains and mixes with the surrounding air. The outer surface of the jet breaks up into very small drops, close to the nozzle exit. As one moves away from the nozzle, the mass of air within

the spray is increases, the spray diverges and the velocity decreases.

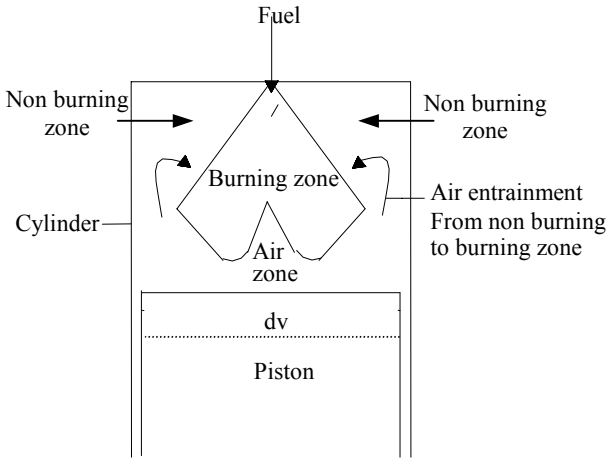

Fig 1. Description of the two zone model

Heat transfer is modeled on a zonal basis and both convective and radiative heat transfer are included. This elaborative approach to modeling heat transfer is based on the fact that heat transfer affects the zone temperature there by the kinetics of pollutant formation. The radiative heat transfer is considered between burning zone and the combustion chamber wall.

Knowing the heat transfer, mass transfer and heat release, the energy equation in conjunction with mass conservation is solved iteratively for each zone to find the zonal temperatures. This provides information such as zone temperature, volume and mass for a fixed cylinder pressure.

Mathematical Treatment

The processes that lead to mixture formation, combustion and pollutant formation are complex and not fully understood so far, thus making simplifying assumptions inevitable.

Assumptions

1.The fuel is injected before the TDC and continues for a definite time interval.

2.Combustion is assumed to take place over a period of crank angle rotation.

3.The combustion chamber is divided into two distinct zones namely burning zone and non burning zone. There is entrainment of air from the burning zone to non-burning zone.

4.Air- fuel ratio assumed to vary as the combustion progresses.

5.Working medium is assumed to be fuel-air-residual mixture with variable specific heat capacities.

6.Combustion products are assumed to be in equilibrium.

7.Effect of spray-wall impingement, air swirl and over lapping are neglected.

Energy balance equation for the non-burning zone gives

$$m_n C_v \frac{dT_n}{d\theta} = -P\frac{dv_n}{d\theta} - \frac{dq_n}{d\theta} - h_a \frac{dm_{ae}}{d\theta} \quad \dots (1)$$

dθ is always taken to be 1°CA, dqn is the heat transfer from the non-burning zone to the cylinder walls and ha is the enthalpy of the air entrained. m_n ,the mass of the non-burning zone is the product of its volume and density of air. Knowing m_n and C_v ,dT_n is calculated.

Energy balance equation for the burning zone gives

$$m_b C_v \frac{dT_b}{d\theta} = -P\frac{dv_b}{d\theta} - \frac{dq_b}{d\theta} + h_a \frac{dm_{ae}}{d\theta} \quad \dots(2)$$

as in the previous case dθ is kept as 1°CA , dqb/dθ is the heat transfer from the burning zone to cylinder walls. m_b, the mass of the burning zone is the cumulative mass of the fuel injected and air entrained. Knowing m_b and C_v dT_b can be calculated.

Thus the average cylinder temperature at any crank angle θ+1, knowing temperature at θ can be given by

$$T(\theta+1) = T(\theta) + \frac{dT_n m_n + dT_b m_b}{m_b + m_n} \dots (3)$$

After the delay period, energy balance equation of non-burning zone is the same as earlier while for burning zone,

$$m_b C_v \frac{dT_b}{d\theta} = \frac{dQ}{d\theta} - P\frac{dV_b}{d\theta} - \frac{dq_b}{d\theta} + h_a \frac{dm_{ae}}{d\theta} \dots(4)$$

where dQ/dθ is the heat release rate which is calculated by using Weibe's function.

$$\frac{dQ}{d\theta} = 6.9\frac{Q_p}{\theta_p}(M_p+1)\left(\frac{\theta}{\theta_p}\right)^{M_p} \exp\left[-6.9\left(\frac{\theta}{\theta_p}\right)^{M_p+1}\right] + 6.9\frac{Q_d}{\theta_d}(M_d+1)\left(\frac{\theta}{\theta_d}\right)^{M_d} \exp\left[-6.9\left(\frac{\theta}{\theta_d}\right)^{M_d+1}\right] \quad \dots(5)$$

where subscripts p and d denote premixed and diffused modes of combustion.

Mp = 3.0 and **Md =0.5** are the shape factors. These values are more or less accepted as universal.

Duration of combustion is determined from following equations:

$\theta_p = 7°CA$

$\theta_d = 0.93Q_d + 24.5$

Qp = 0.5 Qid

where **Qid** is the heat release during delay period

Q d = Qt – Q p,

Where **Qt** is the total energy content of the fuel given by **mf * LCV**

Total duration of combustion is $\theta p + \theta d$

The other aspects of the two-zone model are dealt in detail in the reference [Ganeasan and Anand, 1998]

HEAT TRANSFER MODEL

To study the effect of heat transfer to the coolant a "heat transfer model " is developed. The heat is assumed to be transferred from the combustion chamber to the coolant through the three ways as specified below. Through the cylinder liner, through the cylinder head, through the piston. A steady state heat conduction is assumed for all the above.

Some of the heat generated inside the combustion chamber due to the combustion is transferred to the liner walls by convection and radiation and through the walls by conduction to the coating and by convection to the coolant.

Some of the heat is transferred to the walls of the cylinder head, which is assumed to have constant thickness by convection and radiation and through the walls by conduction and by convection to the coolant. Some of the heat is transferred to the walls of the piston by convection and radiation and from the piston to the liner and from liner to the coating by conduction and from the coating by convection to the coolant. The piston is assumed as a solid cylinder with having an internal node for transfer of heat to the liner. The heat transferred below the piston to the crankcase is neglected. The thermal network for the heat transfer model is shown in the figure 2 and the various resistances shown are

R1 = Resistance for the heat transfer from the combustion chamber to the coolant through liner and coating.

R2 = Resistance for the heat transfer from the combustion chamber to the coolant through the cylinder head.

R3 = Resistance for the heat transfer from the combustion chamber to the coolant through the piston, liner and coating.

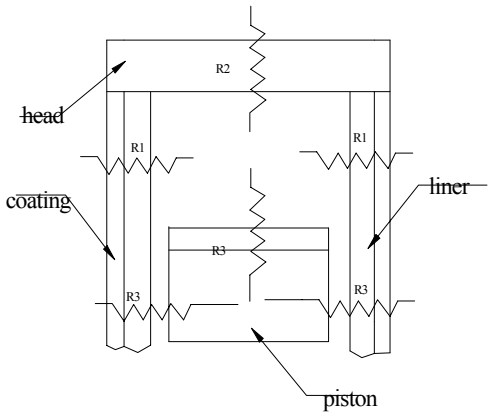

Fig.2.Heat Transfer Model

Heat transfer from the combustion chamber through the liner and the coating is expressed as follows, assuming heat convected and radiated from the gas to the wall is being conducted steadily through the liner walls

$$H h_g 2\pi r_1 (Tg - Tw) + \sigma \varepsilon Ai (Tg^4 - Tw^4) = \frac{Tw - Tc}{\frac{\ln(r_2/r_1)}{2\pi ki H} + \frac{\ln(r_3/r_2)}{2\pi Kc H} + \frac{1}{h_c H 2\pi r_3}} \quad \ldots(6)$$

Similarly the heat transferred through the cylinder head from the combustion chamber is expressed as follows.

$$h_g \pi r_1^2 (Tg - Tw) + \pi r_1^2 \sigma \varepsilon \left(Tg^4 - Tw^4\right) = \frac{Tg - Tw}{\frac{t}{Kh \pi r_1^2} + \frac{1}{h_c \pi r_1^2}} \quad \ldots(7)$$

Similarly the heat transferred through the piston from the combustion chamber is expressed as follows.

$$h_g(\pi r_p^2)(Tg - Tw) + \sigma(\pi r_p^2)\varepsilon\left(Tg^4 - Tw^4\right) = \frac{Tw - Tc}{\frac{1}{Kp\pi Hp} + \frac{1}{h_g Hp 2\pi r_p} + \frac{\ln(r_2/r_1)}{2\pi Ki H} + \frac{\ln(r_3/r_2)}{2\pi Kc H} + \frac{1}{h_c 2\pi r_3 H}} \quad \ldots(8)$$

Where

h_c = Convection Coefficient of coolant
h_g = Convection Coefficient of gas
σ = Bolzman Coefficient
ε = Emmisivity
K_i = Thermal Conductivity of liner
K_c = Thermal Conductivity of coating material
K_h = Thermal Conductivity of cylinder head material
K_p = Thermal Conductivity of piston material
$Ai = 2\pi r_1$ - Surface area of the liner
T_w = Wall Temperature
T_g = Gas Temperature
T_c = Coolant Temperature
H = Distance between piston top and cylinder head
H_p = Height of the piston
t = thickness of the cylinder head
r_1 = inner radius of the liner
r_2 = outer radius of the liner
r_3 = outer radius of the liner + coating thickness
r_p = piston radius

Combining the above three equations 6,7 and 8 a fourth degree equation for Tw is obtained as follows

$A * Tw_4 + B * Tw = C$, Where A, B, C are constants. The above equation is numerically solved to obtain the value of Tw. Initially the gas temperature obtained from the simulation is given as input to the heat transfer model and the value of Tw is obtained as mentioned above. Then with the new wall temperature the gas temperature is recalculated and updated. Iterations are carried out until the difference between the successive values is negligible.

Hence with the help of the above heat transfer model it is possible to simulate the working of the diesel engine with different materials for cylinder head, piston, cylinder liner and different coating materials having different coating thick nesses.

EQUILIBRIUM COMBUSTION PRODUCTS

An estimate of the mole fraction of the products of combustion is essential in calculating the rate of change of internal energy of the system. In order to provide a rapid means of calculation of the equilibrium product mole fraction, a ten species model is used. It specifically deals only with the gas phase combustion products of hydrocarbon fuel with air. The composition is calculated as a function of temperature, pressure and equivalence ratio. Assuming that a fuel with a chemical formula Cα Hβ Oγ Nδ reacts with air at an equivalence ratio Φ, the basic equation limited to ten major species is written as

$$\Phi*\varepsilon*(C_\alpha H_\beta O_\gamma N_\delta) + 0.21*O_2 + 0.79*N_2 \rightarrow \gamma_1 CO_2 + \gamma_2 H_2O + \gamma_3 N_2 + \gamma_4 O_2 + \gamma_5 CO + \gamma_6 H_2 + \gamma_7 H + \gamma_8 O + \gamma_9 OH + \gamma_{10} NO \quad -(6.1)$$

where γ_i is the mole fraction of the product species. Once the solution of the mole fraction is obtained, the specific heat of the gases present inside the cylinder is calculated. The specific heat of the individual product species at a temperature T(K) is given by

$$C_{p,i}/R = a_1 + a_2 T + a_3 T^2 + a_4 T^3 + a_5 T^4$$

where the coefficient 'a' depends on the temperature. The specific heat of the mixture of combustion products is obtained by summing up the product of mole fraction and specific heat of the individual species.

NITRIC OXIDE FORMATION

Although the emitted NOx are mainly composed of nitric oxide(NO) and nitric-dioxide (NO_2), a study of diesel engine emissions can be focused only on NO because its kinetic mechanism is dominant over that of NO_2. The thermal or Zeldovich mechanism consists of two chain reactions. They are

$O + N_2 \leftrightarrow NO + N$,

$N + O_2 \leftrightarrow NO + O$

Zeldovich mechanism can be extended as

$N + OH \leftrightarrow NO + H$

In general, NOx formation is coupled to combustion chemistry through formation of O, OH, O_2 species. The NO concentration can be predicted by the following relation

$$d[NO]/dt = 2 K_f (K_p p/R_u T)^{1/2} [N_2] [O_2]^{1/2} \quad .. (9)$$

$K_f = 1.8e^{11} * \exp[-38370/T(K)]$ $m^3/Kmol.s$

$K_p = 3.6e^3 * \exp[-31090/T(K)]$ $atm^{1/2}$

$[N_2] = y_{n2} * p/(R_u T)$

$[O_2] = y_{o2} * p/(R_u T)$

RESULTS AND DISCUSSION

A computer simulation is performed incorporating all the above factors and standard procedures for other processes in the cycle simulation. The various values obtained from the simulation are tabulated and the following graphs are drawn from the data thus obtained.

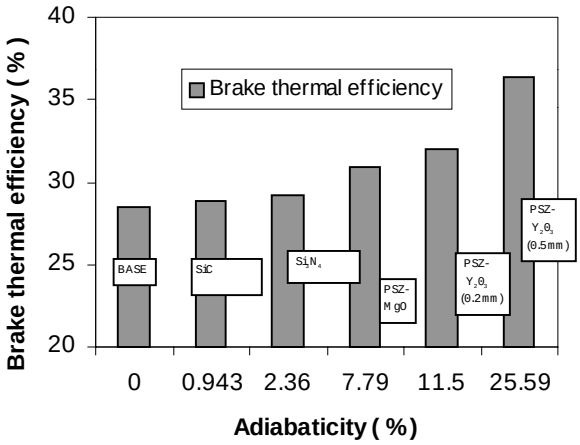

Fig.3 Brake thermal efficiency of the LHR engine with various coating materials

Figure 3 shows the variation of brake thermal efficiency with the adiabaticity. The adiabaticity of the LHR engines are defined as follows:

$$\text{adiabaticity} = \left(\frac{Qb - Qi}{Qb}\right) * 100 \quad , \text{ where}$$

Q_b = heat loss to the coolant of base engine and

Q_i = heat loss to the coolant of insulated engine.

The adiabaticity becomes 100% if the heat loss of the insulated engine becomes zero. It is evident from Figures 3 & 4 that adiabaticity increases as the thermal conductivity (K) of the coating material increases. With the Silicon Nitride as the coating material (thermal conductivity is 10 W/m-K) the adiabaticity that could be achieved is only 2.36% where as with partially stabilized Zirconia with Yittria as the coating material (thermal conductivity is 0.8 W/m-K) the adiabaticity that could be achieved is 25.59%.

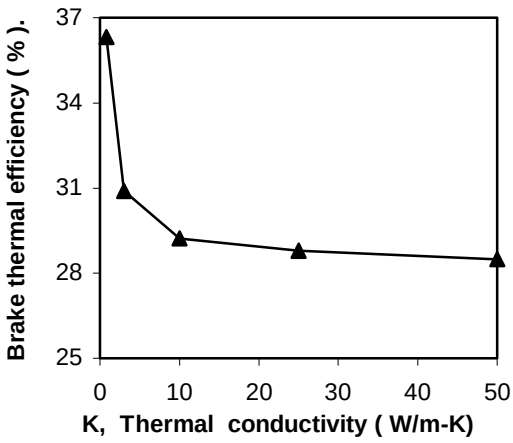

Fig.4 Brake thermal efficiency of the LHR engine with thermal conductivity

The thermal efficiency increases as the adiabaticity increases and thermal conductivity decreases. The thermal efficiency of the base engine is 28.5% and there is around 8% increase in efficiency for the insulated engine with partially stabilized Zirconia with Yittria as the coating material.

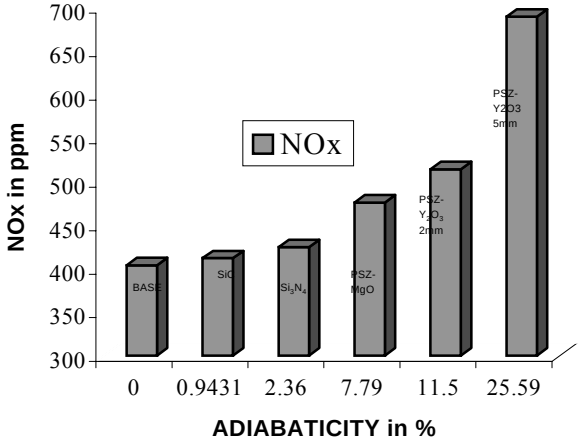

Fig.5 NOx emission of the LHR engine with various coating materials

Figure 5 shows the variation of Nox emission with the adiabaticity. Despite many advantages of the LHR engines the main draw back of them is the emission of Nox. The operating temperatures of the LHR engines are high compared to the normal engines and this contributes to the greater emission of Nox. It is evident from Figure 5 that the NOx predicted increases as the adiabaticity increases which is due to the coating of different materials. The NOx for the base engine is 403 ppm whereas it increases to 686 ppm for the LHR engine whose adiabaticity is 25.59%. This fact necessitates that LHR engines require better emission control techniques as far as the Nox emissions are concerned.

EXPERIMENTAL VALIDATION

In order to validate the results of the simulations and analyze the performance of the LHR engines experiments were conducted on a single cylinder Kirloskar engine (TV1 model). The experimental procedure consists of the following steps. Initially the following tests are conducted on the base engine.

1. The load test or performance test of the base engine under different loading conditions.
2. The heat balance test at different loads.
3. The emission test measuring Oxides of Nitrogen.

The base engine is converted into a low heat rejection engine by replacing the cylinder head and the liner with a new head and a liner coated with 0.5 mm of PSZ and the same set of experiments are conducted as mentioned above in order to compare the performance of the base engine with the low heat rejection engine.

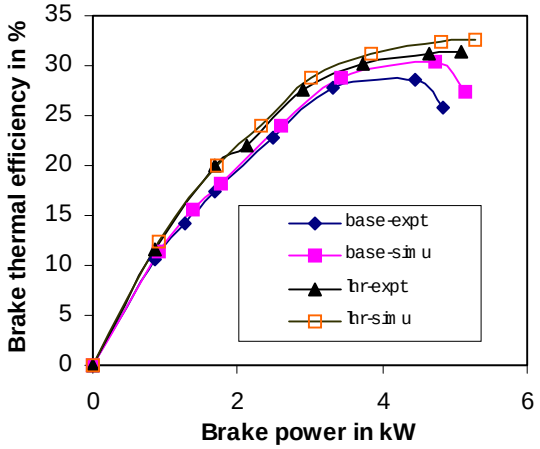

Fig.6 Comparison of Brake Thermal Efficiency of Base engine and LHR Engine.

Figure 6 shows the experimental and predicted brake thermal efficiency with the brake power for both base and LHR engine. The efficiency of the LHR engine is more compared to the base engine for the entire output range, which is highly advantageous as for as the part load operations are concerned

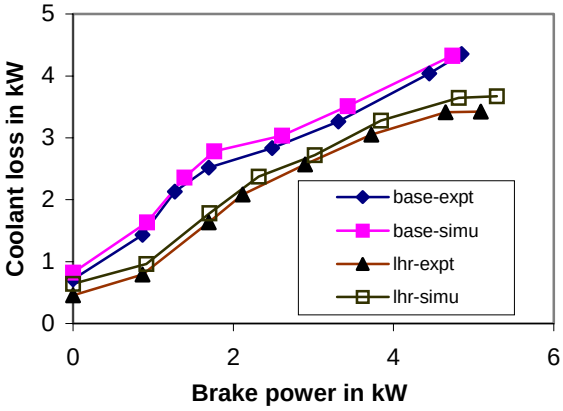

Fig. 7 Comparison of coolant heat loss for Base engine and LHR Engine.

. The maximum efficiency obtained based on the experiments for the base engine is 28.65% at 4.45 kW brake power whereas it is 31.37% for the LHR engine at 5.09 kW. The simulated values agree well with the experimental values within 5 percent.
Figure 7 shows the coolant heat loss in kW for the base engine as well as the LHR engine for the entire load range. As expected the coolant loss is less for the LHR engine compared to the base engine for the entire load range due to the introduction of a thermal barrier coating at the liner and piston head.

Figure 8 shows the exhaust heat loss in kW for the base engine as well as the LHR engine. Significantly the exhaust loss is more for the LHR engine compared to the base engine for the entire load range due to the higher operating temperature prevailing inside the combustion chamber. This leads to an important conclusion that though the coolant heat loss is less for the LHR engine, all the heat is not converted in to useful work output. Substantial portion of the heat find its way to the atmosphere as the exhaust heat loss. However by incorporating heat recovery systems in the exhaust such as turbo compounding the efficiency of the LHR engines can be increased to a higher value.

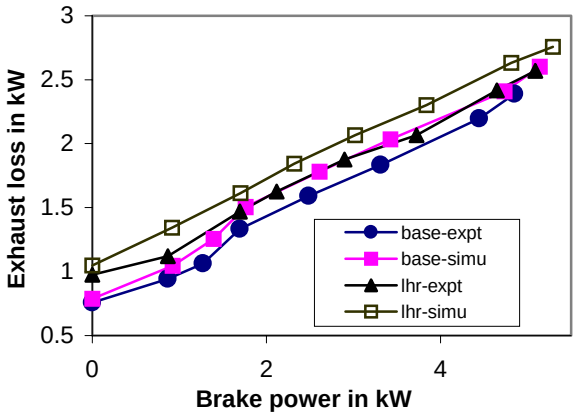

Fig. 8 Comparison of exhaust heat loss for Base engine and LHR Engine.

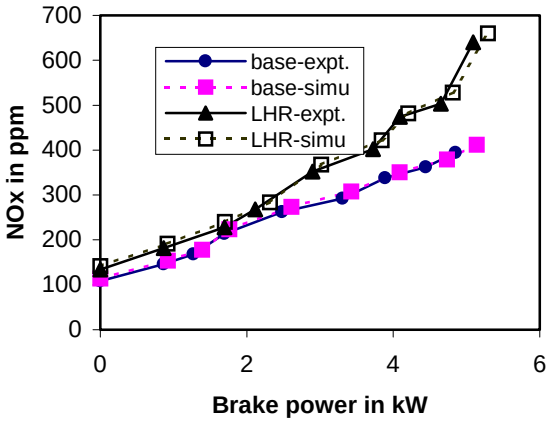

Fig. 9 Variation of NOx with engine Brake power.

Figure 9 shows the emission of Nox for the base engine as well as the LHR engine coated with 0.5 mm thickness of PSZ-Yttria. It is found that the Nox emitted by the LHR engine is high compared to the base engine for the entire load range. For example the Nox emitted for the base engine at no load is 108ppm and at 4.85 kW it is 394 ppm where as the corresponding values for the LHR engine are 134 and 640 ppm respectively. It is alsoto be noted that the simulations closely predict the values both for the base engine as well as the LHR engine.

CONCLUSION

This work has succeeded in predicting the performance of a Low Heat Rejection Direct Injection Diesel Engine with reasonable accuracy. Four simulation studies were performed with different coating materials, Silicon Carbide, Silicon Nitride, PSZ with the Magnesium Oxide and PSZ with Yttrium. The results of the simulation has been validated by conducting experiments on a single cylinder (Kirloskar TV1) engine and on the same engine coated with 0.5 mm thickness of PSZ with Yttria.

REFERENCES

Ganesan and Anand “Combustion models for direct injection diesel engines: A review, comparison and analysis”. Journal of the Institution of Engineers (India) vol.78, (Feb 1998).

Godfrey,D.J., “ Silicon Nitride Ceramics for Engineering Applications” SAE paper740238, 1974.

Jaroslav Wurm, John A Kinast, and Tytus Bulicz “ Assessment of positive Displacement supercharging and Compounding of Adiabatic Diesel” SAE paper840430, 1984.

Jeffrey Carr and Jack Jones “ Post Densified $Cr_2 O_3$ Coatings for adiabatic Engine” SAE paper840432, 1984.

Melvin E. Woods “Ceramic Insulating Components for the Adiabatic Engine”,1984.

Roy Kamo, Walter Bryzik, “ Cummins- TARADCOM Adiabatic Turbo compound Engine Program”. SAE paper 810070,1981.

Sekar, R.R., Kamo, R., and Wood, J.C., “Advanced Adiabatic Diesel Engine for Passenger Cars” SAE paper 840434,1984.